Received: 23 March 2023 | Revised: 15 August 2023 | Accepted: 18 September 2023

DOI: 10.1002/bip.23566

ARTICLE

Biopolymers WILEY

Polymer properties of softwood organosolv lignins produced in two different reactor systems

Prajin Joseph[1] | Mihaela Tanase-Opedal[2] | Størker T. Moe[1]

[1]Department of Chemical Engineering, Norwegian University of Science and Technology (NTNU), Trondheim, Norway

[2]RISE PFI, Trondheim, Norway

Correspondence
Størker T. Moe, Department of Chemical Engineering, Norwegian University of Science and Technology (NTNU), Trondheim, Norway.
Email: storker.moe@ntnu.no

Present address
Prajin Joseph, Borregaard, Sarpsborg, Norway.

Funding information
Norwegian Biorefinery Laboratory, Grant/Award Number: 226247; Norwegian Research Council – Norwegian Centre for Sustainable Bio-based Fuels and Energy (Bio4Fuels), Grant/Award Number: 257622

Abstract

Lignin, the second most abundant biopolymer on earth and with a predominantly aromatic structure, has the potential to be a raw material for valuable chemicals and other bio-based chemicals. In industry, lignin is underutilized by being used mostly as a fuel for producing thermal energy. Valorization of lignin requires knowledge of the structure and different linkages in the isolated lignin, making the study of structure of lignin important. In this article, lignin samples isolated from two types of reactors (autoclave reactor and displacement reactor) were analyzed by FT-IR, size exclusion chromatography, thermogravimetric analysis (TGA), and Py-GC-MS. The average molecular mass of the organosolv lignins isolated from the autoclave reactor decreased at higher severities, and FT-IR showed an increase in free phenolic content with increasing severity. Except for molecular mass and molecular mass dispersity, there were only minor differences between lignins isolated from the autoclave reactor and lignins isolated from the displacement reactor. Carbohydrate analysis, Py-GC–MS and TGA showed that the lignin isolated using either of the reactor systems is of high purity, suggesting that organosolv lignin is a good candidate for valorization.

KEYWORDS
infrared spectroscopy, Organosolv lignin, Organosolv pretreatment, pyrolysis-GC–MS, size exclusion chromatography, thermogravimetric analysis

1 | INTRODUCTION

Lignin is assumed to be the second most abundant polymer in biomass.[1] The amount of lignin in biomass varies between 18% and 33% in softwood, 15%–35% in hardwood, and 5%–30% in herbaceous crops.[2] In bio-based industry, lignin is being used as an energy source, leaving the polymer underutilized.[3] Around 50–70 million tons of lignin is produced annually by the pulp and paper industry and the amount is projected to be around 225 million tons by year 2030.[4] Being an aromatic compound, lignin has the potential to be a raw material for bio-based materials, fuels, and valuable chemicals.[5,6] Lignin has been considered as a low-cost raw material in several applications, such as polymer/resin, cement, carbon fibers, forms, epoxy resins, and so on.[7,8] Research has been done on lignin depolymerization to produce platform molecules (benzene, toluene, xylene) for aromatic chemicals.[9–11]

Lignin is composed of three types of monomer units, *p*-hydroxyphenyl (H), guaiacyl (G), and syringyl (S) derived from the monolignols *p*-coumaryl, coniferyl and sinapyl alcohols, respectively. The content of the different units in lignin depends on the type of biomass the lignin is isolated from. Softwoods contain primarily G units, whereas hardwoods have both G and S units. Grass lignins contain H units in

addition to G and S units.[12] The monomers are linked together to form a heterogeneous polymer. The monomers are linked through different linkages such as ether linkages (typically β-O-4 and α-O-4 linkages) and C—C linkages (e.g., 5–5′, β-β′ or β-5).[13–15] β-O-4 is the most abundant dilignol linkage in native lignin, accounting for more than 50% of the linkages.[16,17] The distribution of the linkages is highly dependent on the delignification process and the reaction parameters of the process.[2,17] An ideal delignification process should result in high yield and purity of lignin, but currently existing methods have some challenges when it comes to the delignification such as modification of the native lignin as in the case of the sulfite process and the kraft process.[18] Another main challenge is the repolymerization or condensation of lignin during delignification. The lignin can form C—C linkages during the delignification process, and this condensed lignin is less reactive and causes issues during depolymerization.[19]

Organosolv lignin is attracting attention since the lignin produced by organosolv pretreatment is only very slightly modified.[20] It has also been reported that the homogeneity of organosolv lignin is higher than other technical lignins such as lignosulfonates, kraft lignin, or alkali lignin.[21] Organosolv lignin has been reported to have lower molecular mass than other technical lignins and high chemical purity.[22] The reactivity of organosolv lignin is much higher compared to other technical lignins due to the presence of several reactive side chains.[6]

Organosolv delignification depends on the ability of the organic solvent to chemically fragment the lignin and physically dissolve the fragmented lignin.[23] Delignification occurs through the hydrolysis of lignin-hemicellulose linkages and the fragmentation of lignin by cleavage of α- and β-ether linkages.[24] The α-ether linkages are more easily cleaved than the β-ether linkages, hence the cleavage of the β-ether linkage is known as the rate-limiting step in organosolv delignification.[25] An unwanted condensation reaction can occur during the delignification, especially under acidic conditions.[26] The condensation reaction is believed to occur when the benzylic carbocation intermediate interacts with an electron-rich carbon atom of a neighboring molecule forming a C—C bond which is very difficult to break, causing the molecular mass of lignin to increase and making valorization of lignin difficult.[23,24]

As mentioned, the type of delignification process influences the structure and purity of isolated lignin. This heterogeneity in lignin structure necessitates the need of lignin characterization prior to lignin valorization. Several analytical methods like fourier-transform infrared spectroscopy (FTIR), size exclusion chromatography (SEC), thermogravimetric analysis (TGA), nuclear magnetic resonance (NMR), and wet chemical analyses have been used to determine the structure, quality, and reactivity of isolated lignins. FTIR has been used to determine functional groups like carbonyl groups, aromatic structures, aliphatic, and aromatic C—O bonds, and the substitution patterns of the aromatic ring.[27–30] TGA is a frequently used method for studying the kinetics of lignin thermal degradation,[31] and this analysis can also be used for estimating the purity of the lignin as carbohydrate impurities devolatilize at lower temperatures than the lignin.[32] Several methods are available for the determination of molecular mass of lignin such as vapor pressure osmometry, ultrafiltration, and SEC.[33–35] Over the last years, the popularity of SEC has increased due to short sample process time, small quantity of sample used, and the broad range of molecular mass detected.[36] For lignin structural analysis, wet chemical methods like for example thioacidolysis[37] have traditionally been used, but nuclear magnetic resonance techniques like ^{31}P-NMR,[37] ^{13}C-NMR,[38] or ^{1}H-NMR[39,40] have shown to be powerful tools for structural elucidation of lignin.

Laboratory studies on delignification are commonly performed using autoclave reactors, where the biomass is cooled together with the spent cooking liquor. This can lead to redeposition of dissolved lignin onto the pretreated material, as shown by for example Joseph et al.[41] who showed that the morphology of organosolv-pretreated biomass depends on the type of reactor system employed (autoclave or displacement). The difference in morphology was attributed to redeposition of lignin onto the fiber surface during cooling down of the autoclave reactor. Another approach to laboratory delignification is the use of flow-through reactors. The "High Pressure Rapid Heating Displacement Pretreatment Reactor" described by Toven et al.[42] is designed with the option to displace the spent cooking liquor with fresh cooking liquor and/or wash liquor, thus reducing the extent of temperature-induced reprecipitation. In this reactor, extensive lignin reprecipitation on the fiber surface did not occur, as opposed to what was observed for conventional autoclave reactors.[41]

The major difference between pretreatment in an autoclave reactor system and in a displacement reactor is that the latter gives the opportunity to displace the spent pretreatment liquor before cooling down the system. This prevents lignin redeposition onto the fiber surfaces due to decreased lignin solubility at lower temperatures.[41]

Due to the difference in lignin redeposition in the two reactor systems, it was considered of interest to investigate whether the redeposition is non-specific or specific. If redeposition is specific, this could lead to different chemical and/or physical properties of organosolv lignins isolated using a displacement reactor compared to lignins isolated using an autoclave reactor. In addition, investigating organosolv effluent lignins (OELs) obtained at different severities could give further information about the properties of lignins from the two types of reactors.

2 | MATERIALS AND METHODS

2.1 | Raw materials and chemicals

The wood chips used in this study were industrial Norway spruce (*Picea abies*) chips from Norske Skog Skogn, Norway. The chips were dried and fractionated to different particle sizes at RISE PFI. The −8/+7 mm fraction was stored at room temperature until further use. A sample of the chips was taken out for chemical analysis, and the chemical composition of the chips is given in Table 1. Absolute ethanol was obtained from VWR chemicals. Sulfuric acid (ACS reagent, 95%–98%), $Ca(OH)_2$, mannitol (ACS reagent, ≥98%), dimethyl

sulfoxide (DMSO), LiBr, and polyethylene glycol (PEG) were obtained from Sigma-Aldrich. All the chemicals were used as received.

A 63% (wt/wt) ethanol–water mixture was used as the solvent in all the reactions and 1% H_2SO_4 (wt/wt, on an oven dried wood basis) was used as catalyst. The cooking liquor composition was based on previous studies.[41,43,44]

2.2 | Moisture content determination

The moisture content of the wood chips was determined gravimetrically. A pre-weighed amount of chips was oven-dried at 105°C overnight and then weighed again. The purpose of determining the moisture content was to ensure accurate loading of wood, water, and chemicals into the reactors.

2.3 | O-factor calculations

The O-factor[43] is analogous to the well-known H factor[45] used in kraft pulping and was used to express the severity of biomass pretreatment as the O-factor takes into account also the heating-up phase of the pretreatment as opposed to the severity factor[46] which only takes into account the time at cooking temperature. The O-factor for the pretreatments was calculated by numerical integration of the recorded temperature profile:

$$O = \int_0^t A e^{-\frac{E_A}{RT}} dt \quad (1)$$

where $E_A = 96$ kJ mol^{-1} and A is chosen so that $Ae^{-\frac{E_A}{RT}} = 1$ at 100°C.

TABLE 1 Chemical composition of the raw material.

	Content, g/100 g
Glucan	43.8
Mannan	10.8
Galactan	1.4
Xylan	4.7
Arabinan	1.1
Lignin (AIL+ASL)[a]	31.5
Extractives	1.0
Ash	0.2
Sum[b]	94.5

[a]AIL, acid-insoluble lignin; ASL, acid-soluble lignin.
[b]The analysis procedure does not quantify uronic acids or acetyl substituents on the hemicellulose, thus an analysis yield somewhat lower than 100% is expected.

2.4 | Autoclave reactor pretreatment

The reactor used in these experiments was a custom-made autoclave reactor system with six parallel autoclaves from TOP industries, France. Each autoclave has an internal volume of 1 L and the system uses electrical heating. The maximum operating pressure and temperature are 50 bar and 220°C. The autoclaves and the caps are manufactured from corrosion-resistant steel (Hastelloy C276) and the autoclave cap is fitted with a thermocouple which extends to the inside of the autoclave. During pretreatment, the autoclaves are seated in an inclined position in the heating unit and are agitated by oscillating rotation of the autoclaves, since the liquor ratios normally used in lignocellulosic biomass pretreatment do not allow for internal agitation.

After transferring an accurately determined amount of chips to the autoclaves, the amount of ethanol and water required to reach 63% (wt/wt) and a liquid-to-biomass ratio of 7.5:1 (volume of liquid:dry mass of biomass) was calculated. The ethanol–water mixture was then added the appropriate amount of H_2SO_4, and the ethanol/water/acid solution was added to the autoclaves. The cap was closed, and the autoclaves were put in the heating unit at a heating rate of 2°C/min. The cooking temperatures and times, and the corresponding severities expressed as the O-factor[43] for the samples are given in Table 2. After the reaction, the autoclaves were cooled in a water bath before separating the cooking liquor and the biomass. The biomass was subsequently washed thoroughly with water, and both cooking liquor and biomass samples were stored at 4°C before analysis.

2.5 | Displacement reactor pretreatment

The displacement reactor is a state-of-the-art reactor setup with the provision of displacing the cooking liquor with fresh solvent without cooling down the reactor. It is a flow-through batch reactor with oil heating allowing for high heating rates if desired, however a heating rate of 2°C per minute was used to match the heating rate of the autoclave reactor. The reactor is equipped with temperature probes located at the bottom (liquor inlet) and top (liquor outlet) of the

TABLE 2 Pretreatment temperatures, time at temperature and O-factors for the autoclave pretreated samples.

	A115	A130	A190	A230	A280
Cooking temperature, °C	150	160	170	180	195
Time to temp, min	59	66	70	76	83
Time at temp, min	167	97	73	44	18
Calculated O-factor	116	129	191	229	280

reactor. For O-factor calculations, the temperature profile recorded at the reactor top (liquor outlet) was used.

The biomass was placed in the reactor and the cooking liquor was pumped to the reactor from a liquid storage tank. The cooking liquor was recirculated throughout the reaction to assure proper mixing and an even temperature distribution. The cooking temperatures and times, and the corresponding severities expressed as the O-factor[43] for the samples are given in Table 3.

After the reaction, the cooking liquor was displaced by fresh cooking liquor at the cooking temperature, and the spent cooking liquor was collected for further analysis. After displacement of the spent cooking liquor with fresh cooking liquor, the biomass was further washed in situ using an ethanol–water mixture of the same concentration as the solvent used for pretreatment, but with no added acid catalyst. This displacement and washing virtually eliminated lignin redeposition onto the fibers.

2.6 | Lignin analysis and preparation

Lignin analysis of the pretreated biomass samples was carried out based on the NREL method for structural carbohydrate and lignin analysis in biomass.[47]

OEL was prepared by precipitating the lignin from the effluent by the addition of three volumes DI water. The precipitated lignin was then filtered using a Whatman GF/A glass microfiber filter and the lignin was washed with water until no change in filtrate color was observed. After washing, the lignin was air-dried to a moisture content of approximately 3%.

The carbohydrate content of the OEL was analyzed by the NREL method[47]: 300 ± 10 mg of OEL was mixed with 3 mL 72 (wt/wt) % H_2SO_4 and incubated at 30°C in a laboshaker for 1 h. After 1 h, the mixture was diluted to 4% H_2SO_4 by addition of 84 mL DI water. The mixture was then autoclaved for 1 h at 121°C. After autoclaving, the mixture was diluted to 140 mL by adding 53 mL DI water and filtered. The filtrate was collected, neutralized with $Ca(OH)_2$ and analyzed by HPLC.

2.7 | High pressure liquid chromatography

The hydrolysates from the pretreated biomass samples and from the organosolv lignin samples were analyzed for monosaccharides on a Shimadzu Providence HPLC system provided with RI and multichannel UV–VIS detectors. Separation was done isocratically on an Agilent Hi-Plex Pb column (300 and 7.8 mm) with an inline deashing column (Bio-Rad Micro-Guard) using DI water as mobile phase. The flow rate was 0.6 mL/min and the column temperature was 50°C.

2.8 | Size exclusion chromatography

The molecular mass distribution of the lignin samples was determined by SEC in an Agilent Isocratic GPC/SEC System with GPC/SEC software. The column system consisted of two Agilent Polargel M columns (7.5 × 300 mm, 8 µm particle size) in series, with an Agilent Polargel M guard column (7.5 × 50 mm, 8 µm particle size) and using dimethyl sulfoxide (DMSO) as the mobile phase. Run time was 30 min. Molecular mass calibration was done using PEG standards. The lignin samples were dissolved in DMSO with 0.1% LiBr and filtered before injection into the instrument.

The data obtained from the SEC analysis were used to calculate the number-average molecular mass ($\overline{M}_n$) and the mass-average

TABLE 3 Pretreatment temperatures, time at temperature and O-factors for the displacement reactor pretreated samples.

	D360	D390	D480
Cooking temperature, °C	188	195	210
Time to temp, min	96	80	80
Time at temp, min	26	76	91
Calculated O-factor	358	388	478

TABLE 4 Outcome of the pretreatment experiments.

				Biomass lignin content, g/100 g[b]		OEL apparent molecular mass, kDa	
Sample	Reactor type	O-factor	Lignin redeposition?[a]	AIL	ASL	$\overline{M}_w$	$\overline{M}_n$
A115	Autoclave	116	None	19.9	0.29	17.1	5.7
A130	Autoclave	129	None	19.4	0.25	17.2	6.0
A190	Autoclave	191	Moderate	14.6	0.33	15.1	5.5
A230	Autoclave	229	Extensive	12.4	0.40	6.5	3.2
A280	Autoclave	280	Extensive	11.2	0.34	5.2	2.8
D390	Displacement	388	None	13.6	0.16	17.2	6.7
D480	Displacement	478	None	9.7	0.15	15.4	5.8
D360	Displacement	358	Slight	5.6	0.29	14.2	6.0

[a]See also Joseph et al.[41]

[b]AIL, acid-insoluble lignin; ASL, acid-soluble lignin.

molecular mass ($\overline{M}_w$) of lignin samples according to Equations (2) and (3), respectively:

$$\overline{M}_n = \frac{\sum_i N_i M_i}{\sum_i N_i} \quad (2)$$

$$\overline{M}_w = \frac{\sum_i m_i M_i}{\sum_i m_i} = \frac{\sum_i N_i M_i^2}{\sum_i N_i M_i} \quad (3)$$

The molecular mass dispersity ($Đ_M$) is defined[48] as the ratio of $\overline{M}_w$ to $\overline{M}_n$:

$$Đ_M = \frac{\overline{M}_w}{\overline{M}_n} \quad (4)$$

2.9 | Attenuated total reflectance fourier-transform infrared spectroscopy

Attenuated total reflectance fourier-transform infrared spectroscopy (ATR-FTIR) spectra were recorded on a PerkinElmer Spectrum 3 with a Universal ATR Sampling Accessory. The lignin samples were air-dried to a moisture content of approximately 3% prior to analysis. In-software correction for residual water was done. The spectra were baseline corrected using the instrument's built-in option and were normalized on the aromatic skeletal vibration band around 1510 cm^{-1}.

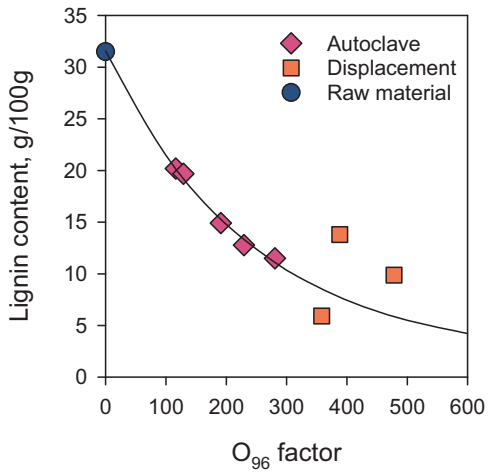

FIGURE 1 Lignin content of the raw material and the pretreated samples. For the autoclave reactor samples, there is a clear and systematic reduction in acid-insoluble lignin in the pretreated samples as the severity of the reaction is increased, however this trend is not seen for the displacement reactor samples. The variability in lignin content versus calculated O-factor for the displacement reactor samples may be attributed to heat transfer limitations. Due to the unsystematic variation in lignin content versus O-factor for the displacement reactor samples, the content of acid-insoluble lignin in the pretreated samples was chosen as the enumerator of the reaction severity.

2.10 | TGA-DSC analysis

TGA was performed on a NETZSCH STA 449 F3 Jupiter instrument using a TGA-DSC socket. A steady flow of nitrogen (40 mL min^{-1}) was employed to maintain an inert atmosphere. Around 10 mg of lignin was loaded to an 85 µL Al_2O_3 crucible. The analysis was done in five stages. Stage 1: heating to 105°C at a heating rate of 5°C/min, Stage 2: Isothermal at 105°C for 10 min, Stage 3: cooling down to 35°C at a rate of 20°C/min, Stage 4: hold at 35°C for 30 min, Stage 5: heating to 800°C at a rate of 5°C/min. The first four stages were for removing all moisture from the samples, and the data from stage 5 were used for analysis.

2.11 | Pyrolysis-GC–MS

The lignin samples were characterized using pyrolysis-GC/MS (pyrolysis-gas chromatography/mass spectrometry). Samples were dried at room temperature and crushed in a mortar before analysis. The samples, about 1 mg, were heated in a reactor from Frontier

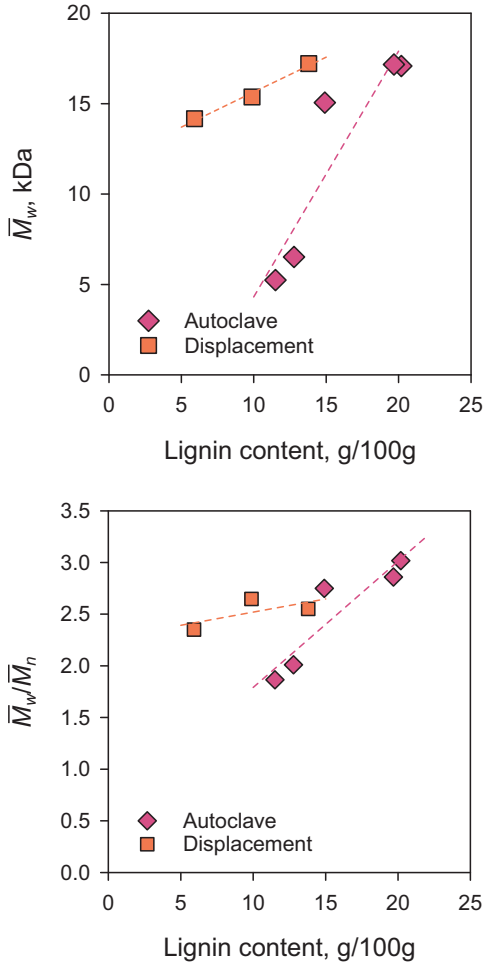

FIGURE 2 (a) Apparent molecular mass and (b) molecular mass dispersity of the organosolv lignins versus the lignin (AIL+ASL) content of the pretreated samples.

Lab (3050TR) at 600°C for 1 min using helium as the carrier gas. The samples were carried on to an Ultra ALLOY-1 capillary column (Frontier, 30 m-0.25 mm id, 2.0 µm film) fitted in a GC 7890B (Agilent Technologies) set in split mode (50:1). The temperature was held at 35°C for 5 min, then increased by 15°C/min to a final temperature of 300°C and held at 300°C for 5 min. Eluting compounds were detected with a 5977B MSD mass spectroscopy detector (Agilent Technologies). The mass range was from 14 to 550 *m/z* and total ion chromatograms (TIC) were reconstructed. The compounds were identified from their mass spectra by comparison with spectra in library databases.

3 | RESULTS AND DISCUSSION

The outcome of the organosolv pretreatments is given in Table 4. As there was some variation in heat-up time and temperature overshoot between the different pretreatments, the O-factor[43] rather than the severity factor[46] was chosen for enumeration of the pretreatment severity, as the severity factor only considers time at constant temperature and not the effect of varying temperature on the reaction rate.[46]

While the autoclave reactor biomass samples showed varying degree of lignin redeposition onto the fiber surface, the displacement reactor biomass samples showed no or very slight redeposition onto

TABLE 5 Assignment of observed IR absorption peaks in softwood lignin.[56–58]

Peak number	Wavenumber, cm^{-1}	Peak assignment
1	3434	O—H stretching
2	2939	C—H stretching
3	1717	C═O stretching in conjugated ketones and carboxylic groups
4	1595	C═C aromatic ring vibration
5	1511	Aromatic skeletal vibration
6	1464	C—H deformation in $—CH_3$ and $—CH_2—$
7	1423	Aromatic skeletal vibrations
8	1372	Phenolic OH and aliphatic C—H
9	1269	C—O of guaiacyl (G) ring
10	1217	C—O and glucopyranoic symmetric vibration
11	1136	C—O—C stretching and symmetric vibration of the ether linkage
12	1089	Aromatic C—H in-plane deformation in the guaiacyl ring
13	1032	C—O deformation in primary alcohols
14	855	Aromatic out-of-plane deformation

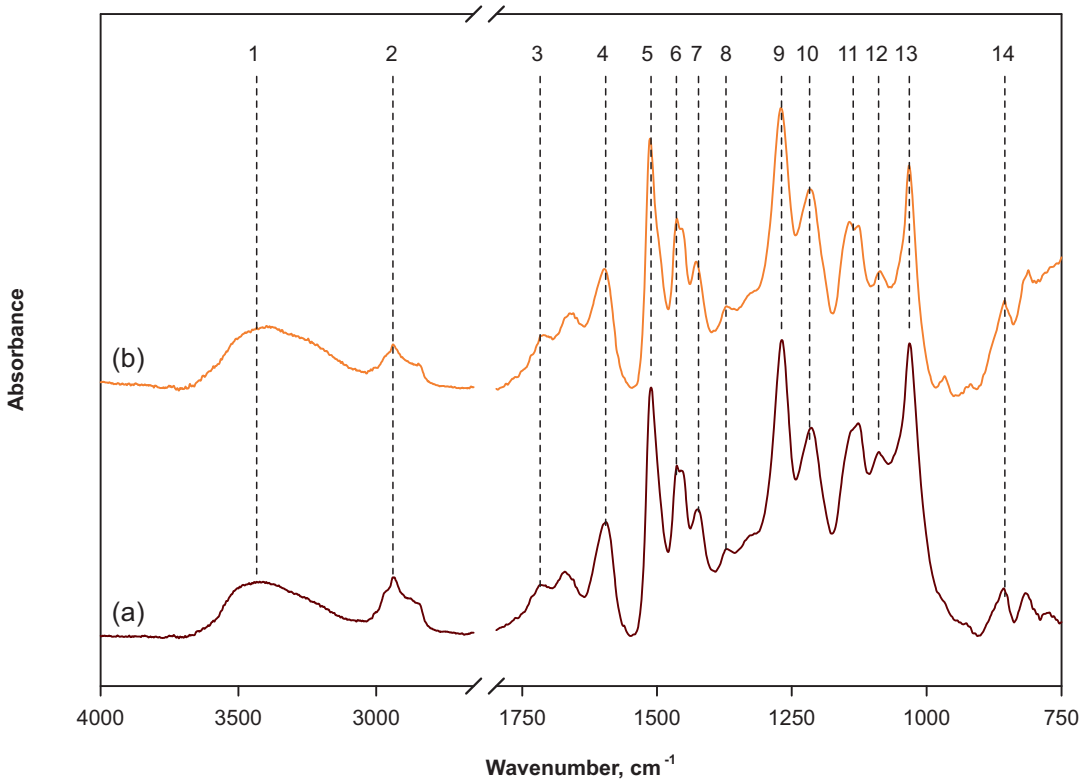

FIGURE 3 Comparison of FTIR data of lignin samples from (a) the autoclave reactor (sample A190, M_w = 15.1 kDa) and (b) the displacement reactor (sample D360, M_w = 14.2 kDa). Numbers above the peaks refer to peak assignments in Table 5.

the fiber surface. However, redeposition was observed in the lumen of the fibers.[41] As expected given the acidic reaction conditions during pretreatment, very low levels of acid-soluble lignin were detected in the pretreated samples. The correlation between the O-factor and the lignin content (AIL+ASL) of the samples is given in Figure 1.

3.1 | Size exclusion chromatography

The apparent molecular mass and molecular mass dispersity of the samples is given in Figure 2. The observed reduction in molecular mass of the organosolv lignins with increased severity for all samples was as expected as it can be safely assumed that as the reaction severity increased, more bond breakage occurred resulting in smaller lignin fragments. However, the large difference in molecular mass dispersity was not expected. At high severities, the autoclave reactor samples show a strong decrease in molecular mass dispersity with increasing severity, approaching $\overline{M}_w/\overline{M}_n = 2$. On the other hand, the displacement reactor samples only showed a slight decrease in molecular mass dispersity. A molecular mass dispersity close to 2.0, as observed for the high-severity treated autoclave samples, is what would be expected from random depolymerization of a high-M polymer.[49,50] One hypothesis could then be that at lower severities specific sites are attacked and bonds are broken resulting in a wide range of fragment size, but as the severity is increased the bond breakage becomes more random resulting in more uniform chain lengths.

However, a more plausible explanation for the observed trend in dispersity is lignin redeposition on the pretreated biomass. It has been shown previously that lignin is redeposited onto the biomass on cooling before washing the biomass,[41] and as seen from Figure 2 and Table 4, the molecular mass dispersity $\overline{M}_w/\overline{M}_n$ decreases with increasing levels of redeposition.

Flory and Huggins[51–55] showed that the entropy of mixing a polymer and a solvent decrease with increasing molecular mass, thus the solubility of a polymer decreases with increasing molecular mass. In a polydisperse polymer sample like partly depolymerized lignin, the high-molecular mass fraction will have the lowest solubility and will thus

TABLE 6 Carbohydrate analysis of lignin sample A130.

Compound	Content, g/100 g
Glucan	0.69
Xylan	0.86
Arabinan	2.99
Galactan	n.d.[a]
Mannan	2.28
Lignin	93.73

[a]Not detected.

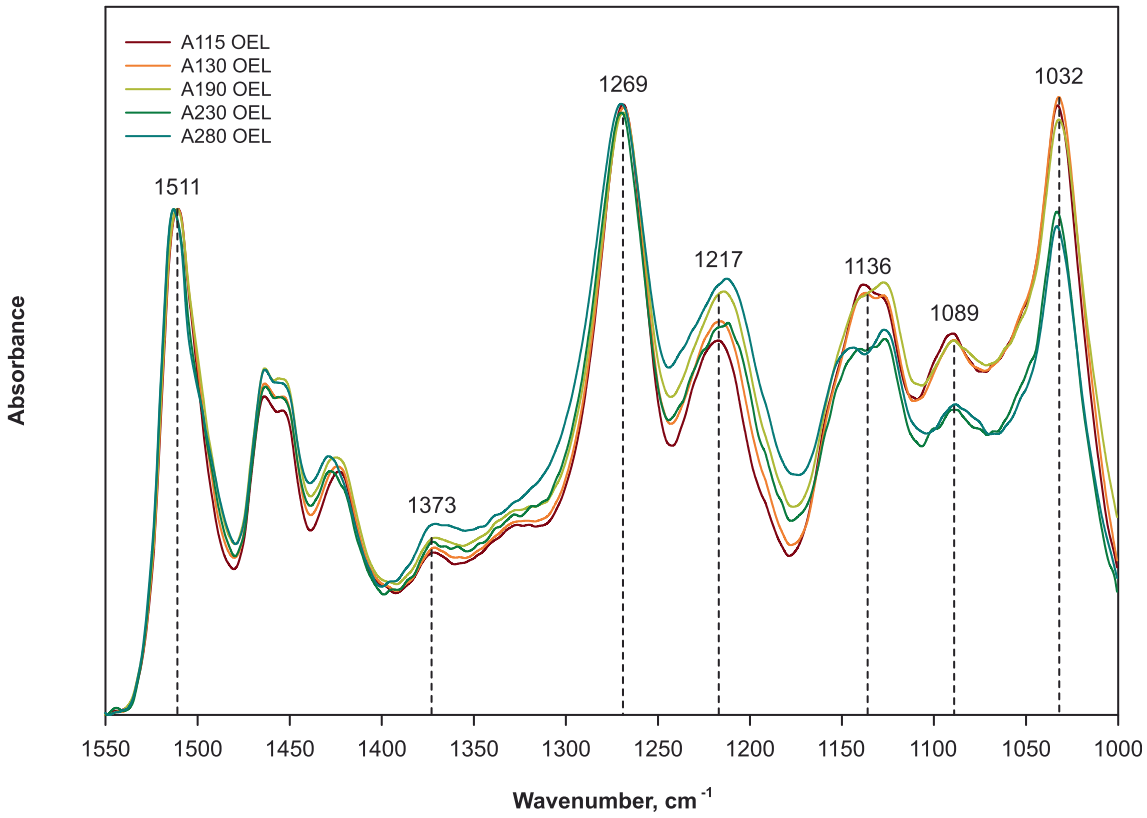

FIGURE 4 Comparison of FTIR data of autoclave samples in the wave number range 1550–1000 cm^{-1}. Spectra have been normalized to identical height of the aromatic skeletal vibrational band at 1511 cm^{-1}.

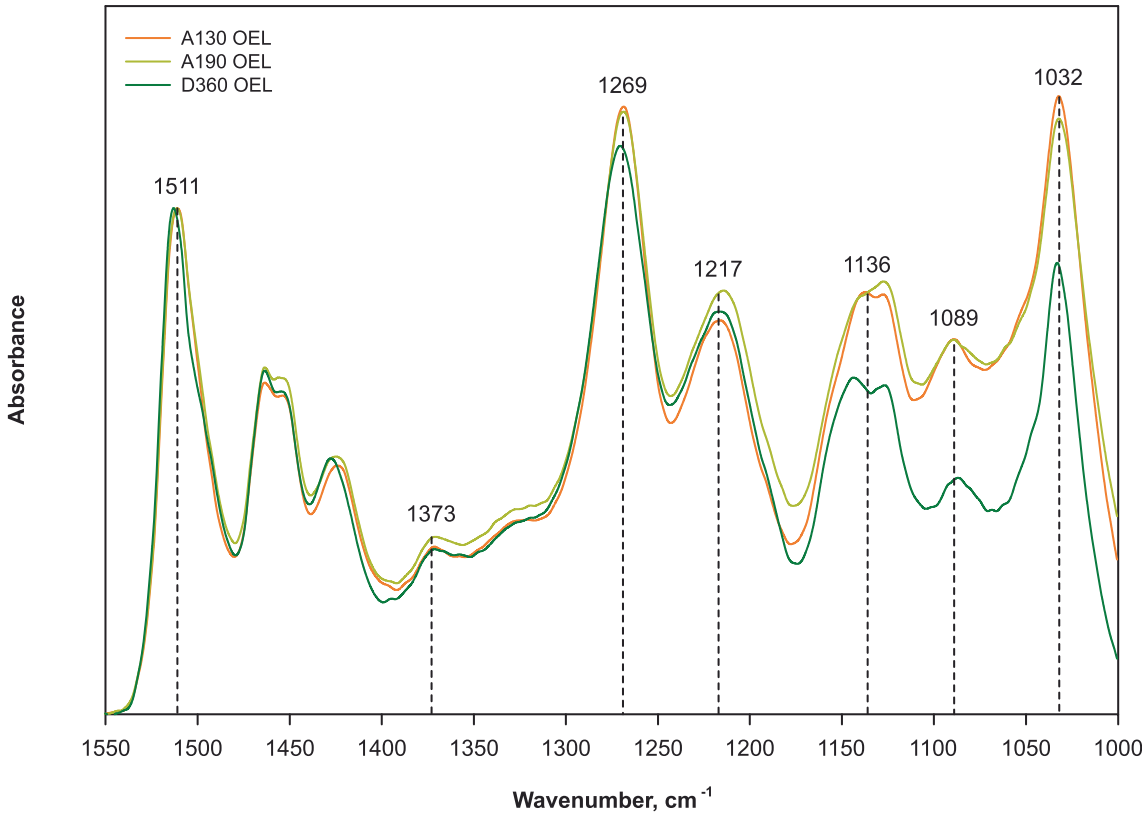

FIGURE 5 Comparison of FTIR data of two autoclave samples and one displacement reactor sample in the wavenumber range 1550–1000 cm^{-1}. Spectra have been normalized to identical height of the aromatic skeletal vibrational band at 1511 cm^{-1}.

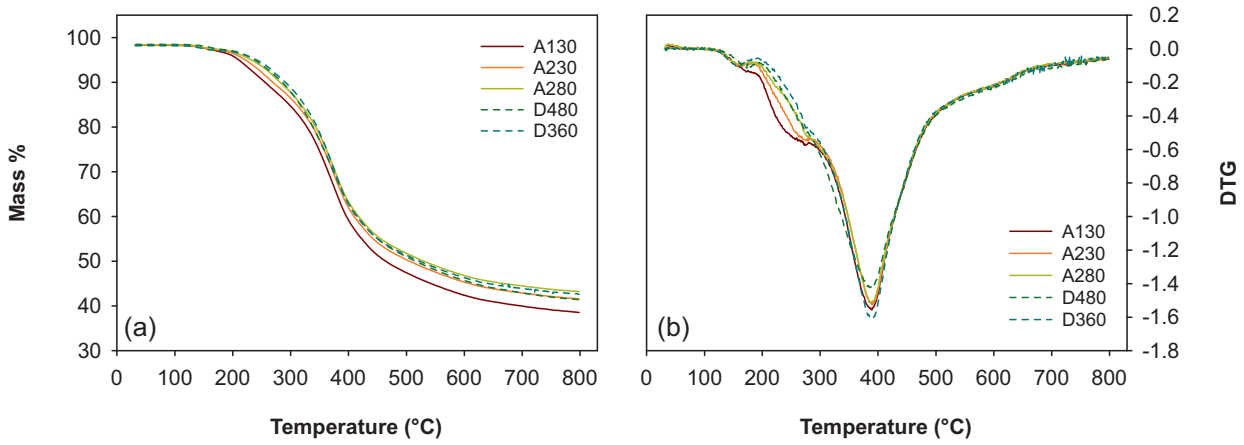

FIGURE 6 (a) Thermogravimetric analysis and (b) DTG curves for selected lignin samples from the autoclave reactor and from the displacement reactor. Samples A130-A280: Autoclave reactor samples, samples D480 and D360: Displacement reactor samples.

preferentially redeposit onto the biomass when the solubility parameters (e.g., temperature) decrease. Since the high-molecular mass fraction is preferentially redeposited, significant lignin redeposition should give a narrower molecular mass distribution and a decreased molecular mass dispersity for the fraction of the polymer still in solution. This is also what was observed; the lowest molecular mass dispersity was observed for the samples where extensive redeposition was observed.

Lignin samples from the displacement reactor had molecular masses (both $\overline{M}_n$ and $\overline{M}_w$) and dispersity similar to those of the low temperature lignin samples from the autoclave reactor. It is assumed that the lack of significant redeposition in the displacement reactor caused the molecular masses and the dispersity to be higher compared to the samples from the autoclave reactor at similar severities.

3.2 | ATR-FTIR

A comparison of FTIR spectra for one autoclave reactor sample and one displacement reactor sample shows strong similarities between the samples, suggesting that the lignin isolated from the two reactors are similar in structure and purity. This comparison is given in Figure 3. Peak assignments are given in Table 5.

A more detailed investigation of the FTIR spectra from the autoclave reactors showed an interesting trend (Figure 4). The phenolic hydroxyl group signal at 1217 cm^{-1} increased and the primary aliphatic alcohol signal at 1032 cm^{-1} decreased with increasing severity/redeposition, indicating an increased breakage of β-O-4 bonds as would be expected for a lower molecular mass lignin. Similarly, and supporting this hypothesis, the signal assigned to C—O—C bond stretching at 1136 cm^{-1} decreased with increasing severity/redeposition. This is consistent with the strong decrease in M_w as severity increased. The peak at 1269 cm^{-1} assigned to guaiacyl C—O is of nearly identical intensity for the autoclave reactor lignins. Comparing these results to the FTIR spectrum of a loblolly pine ethanol organosolv lignin,[59] we see a lower content of C—O—C bonds (1136 cm^{-1}) and a similar content of phenolic OH (1372 cm^{-1}) in our samples. However, as we see varying content of C—O—C bonds and phenolic hydroxyl content with varying severity, it is difficult to compare detailed features between different laboratories when the pretreatment severity and the average molecular mass is not stated.

Comparing one of the displacement reactor lignins (D360, $M_w = 14.2$ kDa, $M_n = 6.0$ kDa) with autoclave lignins with similar apparent number-average or weight-average molecular mass (A130, $M_n = 6.0$ kDa; A190, $M_w = 15.1$ kDa), other differences are seen (Figure 5). The displacement reactor sample shows lower absorbance at 1269, 1136, 1089, and 1032 cm^{-1} (assigned to guaiacyl C—O, C—O—C, guaiacyl C—H and primary alcohol C—O, respectively), however the signal assigned to phenolic OH and to aliphatic C—H is very similar between samples, as should be expected for lignins with similar molecular masses.

3.3 | TGA-DSC analysis

TGA results of selected lignin samples are given in Figure 6. The reduction in mass over time shows a similar trend for all the lignin samples. The samples start to degrade around 200°C and stabilize around 600°C. There is not much thermal degradation after 600°C. The residual amount after the degradation is around 40% of the initial mass taken for analysis. It can be assumed that the reduction in mass between 200 and 300°C is due to the thermal degradation of carbohydrates.[32] The differential thermogravimetric (DTG) analysis shows that the maximum degradation of the samples occurred around 400°C. Carbohydrate analysis of one of the lignin samples (A130, Table 6) showed more than 90% lignin and small amounts of carbohydrates, mainly hemicelluloses. The amount of hemicellulose sugars in the lignin sample agrees with the observed thermal degradation in the range 200–300°C.

A trend toward less thermal degradation in the range 200–300°C (Figure 6b) for lignins isolated at higher severities is interpreted as a somewhat lower carbohydrate content of the lignins with higher

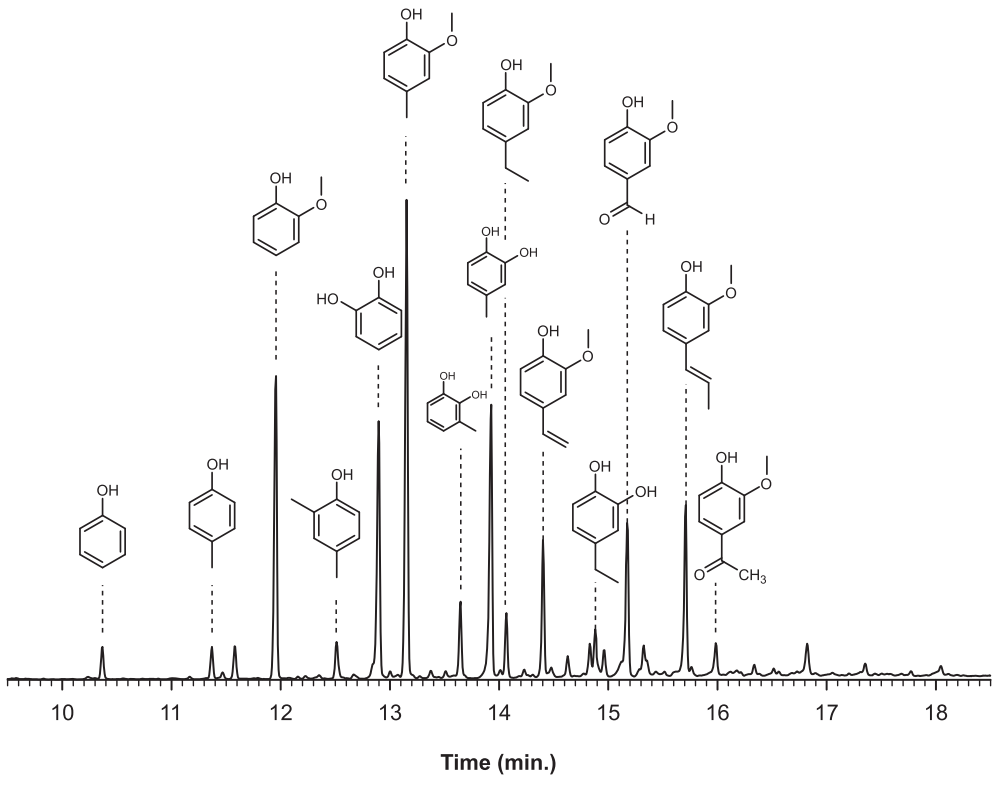

FIGURE 7 Py-GC–MS spectrum of lignin sample A190.

TABLE 7 List of main compounds identified from the Py-GC–MS analysis and their corresponding retention times.

Compound	Retention time, min	Abundance, % of total
Phenol	10.36	1.1
p-Cresol	11.36	1.0
2-Methoxyphenol	11.95	13.6
2,4-Dimethylpenol	12.51	1.4
Cathecol	12.89	12.3
Creosol	13.14	20.4
3-Methyl-1,2-benzenediol	13.64	2.8
4-Methyl-1,2-benzenediol	13.91	12.8
2-Methoxy-4-ethylphenol	14.07	2.3
2-Methoxy-4-vinylphenol	14.40	5.2
Ethylcathecol	14.88	4.2
Vanillin	15.17	7.8
trans-isoeugenol	15.71	7.6
Apocynin	15.99	1.3

severities. Zhou et al.[59] investigated the thermal degradation of lignins from oak, pine, and corn stover and found that the mass loss in the range 200–300°C was highest for the corn stover lignin and lowest for the hardwood lignin. Here, we see that the mass loss in that temperature range decreases with increasing pretreatment severity indicating a lower carbohydrate content of the lignins with increasing severity.

3.4 | Py-GC–MS analysis

Py-GC–MS analysis of the organosolv lignins also showed that most of the compounds identified are degradation products of lignin. A typical pyrolysis chromatogram is shown in Figure 7, and the main compounds identified from the pyrolysis chromatogram are given in Table 7. There was no significant difference in the spectra of samples from the autoclave and the displacement reactor, nor between lignins isolated at different severities. This is consistent with the observation from the TGA analysis and the carbohydrate analysis that the organosolv lignins have a very low content of carbohydrate impurities.

4 | CONCLUSION

Lignins isolated from organosolv pretreatment of Norway spruce in an autoclave reactor system and in a displacement reactor showed small differences except for molecular mass and molecular mass dispersity. All lignin samples appeared to be of high purity and had similar thermogravimetric behavior. The difference in molecular mass and molecular mass dispersity suggests that the high-molecular mass fraction of dissolved organosolv lignin is redeposited onto the biomass upon cooling, consistent with what has been observed previously. Samples from the displacement reactor showed very little relationship between severity, molecular mass and molecular mass dispersity, consistent with no redeposition of the high-molecular mass fraction of the dissolved lignin. The main lignin parameters influenced by the reactor design are molecular mass and molecular mass dispersity.

AUTHOR CONTRIBUTIONS

Prajin Joseph: Conceptualization, formal analysis, investigation, visualization, writing—original draft. **Mihaela Tanase-Opedal:** Conceptualization, supervision. **Størker T. Moe:** Conceptualization, formal analysis, project administration, supervision, visualization, writing—review and editing.

ACKNOWLEDGMENTS

This project was funded by the Department of Chemical Engineering, NTNU, Trondheim. The authors would like to acknowledge RISE PFI for technical assistance and providing the laboratory facilities. This work is carried out as part of the Norwegian national research infrastructure project NorBioLab (Norwegian Biorefinery Laboratory, grant # 226247) and Norwegian Centre for Sustainable Bio-based Fuels and Energy (Bio4Fuels, grant # 257622), and we gratefully acknowledge The Research Council of Norway for financial support. The authors would also like to thank Jost Ruwoldt and Marianne Ø. Dalheim at RISE PFI for the help with SEC data collection and analysis.

FUNDING INFORMATION

Prajin Joseph: NTNU PhD stipend, project # 70441799 and Norwegian Research Council (Norges Forskningsråd) grant # 226247 (Norwegian national research infrastructure project NorBioLab). Mihaela Tanase-Opedal: Norwegian Research Council (Norges Forskningsråd) grant # 257622 (Norwegian Centre for Sustainable Bio-based Fuels and Energy, Bio4Fuels) Størker T. Moe: NTNU internal funding.

CONFLICT OF INTEREST STATEMENT

The authors declare no conflict of interest.

DATA AVAILABILITY STATEMENT

The most relevant data are given in the manuscript's tables. Figure data and temperature profiles of the pretreatments are available as Supporting Information.

ORCID

Prajin Joseph https://orcid.org/0000-0003-1825-8520
Mihaela Tanase-Opedal https://orcid.org/0000-0001-9515-8561
Størker T. Moe https://orcid.org/0000-0001-5100-574X

REFERENCES

[1] S. Gillet, M. Aguedo, L. Petitjean, A. R. C. Morais, A. M. da Costa Lopes, R. M. Łukasik, P. T. Anastas, *Green Chem* **2017**, *19*, 4200.
[2] A. E. Rodrigues, P. C. D. O. R. Pinto, M. F. Barreiro, C. A. E. Da Costa, M. I. F. Da Mota, I. Fernandes, *An Integrated Approach for Added-Value Products from Lignocellulosic Biorefineries*, Springer, Cham **2018**.
[3] H. Wang, Y. Pu, A. Ragauskas, B. Yang, *Bioresour. Technol.* **2019**, *271*, 449.
[4] I. Haq, P. Mazumder, A. S. Kalamdhad, *Bioresour. Technol.* **2020**, *312*, 123636.

[5] W. Schutyser, T. Renders, S. Van den Bosch, S. F. Koelewijn, G. T. Beckham, B. F. Sels, *Chem. Soc. Rev.* **2018**, *47*, 3.
[6] A. Vishtal, A. Kraslawski, *BioResources* **2011**, *6*, 3547.
[7] P. A. Lazaridis, A. P. Fotopoulos, S. A. Karakoulia, K. S. Triantafyllidis, *Front Chem* **2018**, *6*, 6.
[8] R. N. Olcese, J. Francois, M. M. Bettahar, D. Petitjean, A. Dufour, *Energy Fuels* **2013**, *27*, 975.
[9] A. M. Elfadly, I. F. Zeid, F. Z. Yehia, A. M. Rabie, M. M. aboualala, S.-E. Park, *Int. J. Biol. Macromol.* **2016**, *91*, 278.
[10] L. Serrano, J. A. Cecilia, C. García-Sancho, A. García, in *Lignin Chemistry* (Eds: L. Serrano, R. Luque, B. F. Sels), Springer, Cham **2020**, p. 169.
[11] P. Sirous-Rezaei, J. Jae, J.-M. Ha, C. H. Ko, J. M. Kim, J.-K. Jeon, Y.-K. Park, *Green Chem* **2018**, *20*, 1472.
[12] A. Naseem, S. Tabasum, K. M. Zia, M. Zuber, M. Ali, A. Noreen, *Int J Biol Macromol* **2016**, *93*, 296.
[13] S. Constant, H. L. J. Wienk, A. E. Frissen, P. D. Peinder, R. Boelens, D. S. Van Es, R. J. H. Grisel, B. M. Weckhuysen, W. J. J. Huijgen, R. J. A. Gosselink, et al., *Green Chem* **2016**, *18*, 2651.
[14] G. Gellerstedt, G. Henriksson, in *Monomers, Polymers and Composites from Renewable Resources* (Eds: M. N. Belgacem, A. Gandini), Elsevier, Amsterdam **2008**, p. 201.
[15] J.-L. Wen, B.-L. Xue, F. Xu, R.-C. Sun, A. Pinkert, *Ind Crops Prod* **2013**, *42*, 332.
[16] W.-B. Huang, C.-Y. Du, J.-A. Jiang, Y.-F. Ji, *Res. Chem. Intermed.* **2012**, *39*, 2849.
[17] M. P. Pandey, C. S. Kim, *Chem. Eng. Technol.* **2011**, *34*, 29.
[18] T. Aro, P. Fatehi, *ChemSusChem* **2017**, *10*, 9.
[19] T. J. McDonough, *Tappi J.* **1993**, *76*, 186.
[20] E. K. Pye, in *Biorefineries—Industrial Processes and Products*, Vol. 2 (Eds: B. Kamm, P. R. Gruber, M. Kamm), Wiley-VCH, Weinheim **2010**, p. 165.
[21] N.-E. E. Mansouri, J. Salvadó, *Ind Crops Prod* **2006**, *24*, 8.
[22] J. H. Lora, W. G. Glasser, *J. Polym. Environ.* **2002**, *10*, 39.
[23] T. J. McDonough, *The Chemistry of Organosolv Delignification*, Institute of Paper Science and Technology, Atlanta, GA **1992**.
[24] N. Brosse, M. H. Hussin, A. A. Rahim, in *Biorefineries* (Eds: K. Wagemann, N. Tippkötter), Springer, Cham **2017**, p. 153.
[25] M. Meshgini, K. V. Sarkanen, *Holzforschung* **1989**, *43*, 239.
[26] P. Sannigrahi, A. J. Ragauskas, *Aqueous Pretreatment of Plant Biomass for Biological and Chemical Conversion to Fuels and Chemicals*, Wiley, Chichester **2013**.
[27] O. Goldschmid, in *Lignins: Occurrence, Formation, Structure and Reactions* (Eds: K. V. Sarkanen, C. H. Ludwig), Wiley Interscience, New York **1971**, p. 241.
[28] B. Hortling, T. Tamminen, E. Kenttä, *Holzforschung* **1997**, *51*, 405.
[29] D. M. Le, A. D. Nielsen, H. R. Sørensen, A. S. Meyer, *BioEnergy Res* **2017**, *10*, 1025.
[30] J. Lisperguer, P. Perez, S. Urizar, *J. Chil. Chem. Soc.* **2009**, *54*, 4.
[31] J. Zhang, T. Chen, J. Wu, J. Wu, *Bioresour. Technol.* **2014**, *166*, 87.
[32] C. Di Blasi, *Prog. Energy Combust. Sci.* **2008**, *34*, 47.
[33] A. V. Gidh, S. R. Decker, T. B. Vinzant, M. E. Himmel, C. Williford, *J Chromatogr A* **2006**, *1114*, 1.
[34] R. J. A. Gosselink, A. Abächerli, H. Semke, R. Malherbe, P. Käuper, A. Nadif, J. E. G. van Dam, *Ind Crops Prod* **2004**, *19*, 271.
[35] A.-S. Jönsson, A.-K. Nordin, O. Wallberg, *Chem. Eng. Res. Des.* **2008**, *86*, 1271.
[36] A. Tolbert, H. Akinosho, R. Khunsupat, A. K. Naskar, A. J. Ragauskas, *Bioprod Biorefin* **2014**, *8*, 836.
[37] R. J. A. Gosselink, J. E. G. van Dam, E. de Jong, E. L. Scott, J. P. M. Sanders, J. Li, G. Gellerstedt, *Holzforschung* **2010**, *64*, 2.
[38] K. P. Kringstad, R. Mörck, *Holzforschung* **1983**, *37*, 237.
[39] S. Li, K. Lundquist, *Nord. Pulp Pap. Res. J.* **1994**, *9*, 191.
[40] K. Lundquist, in *Methods in Lignin Chemistry* (Eds: S. Y. Lin, C. W. Dence), Springer-Verlag, Berlin **1992**, p. 242.
[41] P. Joseph, V. Ottesen, M. T. Opedal, S. T. Moe, *Biopolymers* **2022**, *113*, e23520.
[42] K. Toven, K. Øyaas, M. Tanase-Opedal, Ø. Eriksen, High Pressure Rapid Heating Displacement Pretreatment Reactor: A unique tool for developing new pretreatment technologies. In 7th Nordic Wood Biorefinery Conference, Stockholm, Sweden, 2017.
[43] P. Joseph, M. T. Opedal, S. T. Moe, *Biomass Convers Biorefin* **2021**, *13*, 6727.
[44] S. Agnihotri, I. A. Johnsen, M. S. Bøe, K. Øyaas, S. Moe, *Wood Sci. Technol.* **2015**, *49*, 881.
[45] K. E. Vroom, *Pulp Paper Mag Canada* **1957**, *58*, 228.
[46] N. Abatzoglou, E. Chornet, K. Belkacemi, R. P. Overend, *Chem. Eng. Sci.* **1992**, *47*, 1109.
[47] A. Sluiter, B. Hames, R. Ruiz, C. Scarlata, J. Sluiter, D. Templeton, D. Crocker, *Determination of Structural Carbohydrates and Lignin in Biomass*, National Renewable Energy Laboratory, Golden, CO **2012**.
[48] R. F. T. Stepto, *Pure Appl. Chem.* **2009**, *81*, 351.
[49] A. Kuhn, *Ber. Dtsch. Chem. Ges.* **1930**, *63*, 1503.
[50] P. J. Flory, *J. Am. Chem. Soc.* **1936**, *58*, 1877.
[51] P. J. Flory, *Principles of Polymer Chemistry*, Cornell University Press, Ithaca **1953**.
[52] P. J. Flory, *J Chem Phys* **1942**, *10*, 51.
[53] M. L. Huggins, *Ann. N. Y. Acad. Sci.* **1942**, *43*, 1.
[54] M. L. Huggins, *J. Phys. Chem.* **1942**, *46*, 151.
[55] M. L. Huggins, *J. Am. Chem. Soc.* **1942**, *64*, 1712.
[56] L. M. Kline, D. G. Hayes, A. R. Womac, N. Labbé, *BioResources* **2010**, *5*, 1366.
[57] T. Rashid, C. F. Kait, T. Murugesan, *Proc Eng* **2016**, *148*, 1312.
[58] R. J. Sammons, D. P. Harper, N. Labbé, J. J. Bozell, T. Elder, T. G. Rials, *BioResources* **2013**, *8*, 2752.
[59] S. Zhou, Y. Xue, A. Sharma, X. Bai, *ACS Sustain Chem. Eng.* **2016**, *4*, 6608.

SUPPORTING INFORMATION

Additional supporting information can be found online in the Supporting Information section at the end of this article.

How to cite this article: P. Joseph, M. Tanase-Opedal, S. T. Moe, *Biopolymers* **2023**, e23566. https://doi.org/10.1002/bip.23566